Cross-Loop Optimization of Arithmetic Intensity for Finite Element Local Assembly

Fabio Luporini, Imperial College London
Ana Lucia Varbanescu, University of Amsterdam
Florian Rathgeber, Imperial College London
Gheorghe-Teodor Bercea, Imperial College London
J. Ramanujam, Louisiana State University
David A. Ham, Imperial College London
Paul H.J. Kelly, Imperial College London

We study and systematically evaluate a class of composable code transformations that improve arithmetic intensity in local assembly operations, which represent a significant fraction of the execution time in finite element methods. Their performance optimization is indeed a challenging issue. Even though affine loop nests are generally present, the short trip counts and the complexity of mathematical expressions, which vary among different problems, make it hard to determine a single or unique sequence of successful transformations. Our investigation has resulted in the implementation of a compiler for local assembly kernels, fully integrated with a real framework for developing finite element methods. The compiler manipulates abstract syntax trees generated from a domain-specific language for partial differential equations by introducing domain-aware optimizations, tailored to instruction-level parallelism and register locality. Eventually, C code including vector SIMD intrinsics is produced. Experiments using a range of finite-element problems of increasing complexity show that significant performance improvement is achieved. The generality of the approach and the applicability of the proposed code transformations to other domains is also discussed.

1. INTRODUCTION

In many fields such as computational fluid dynamics, computational electromagnetics and structural mechanics, phenomena are modelled by partial differential equations (PDEs). Numerical techniques, like the finite volume method and the finite element method, are widely employed to approximate solutions of these PDEs. Unstructured meshes are often used to discretize the computational domain, since they allow an accurate representation of complex geometries. The solution is sought by applying suitable numerical operations, or kernels, to the entities of a mesh, such as edges, vertices, or cells. On standard clusters of multicores, typically, a kernel is executed sequentially by a thread, while parallelism is achieved by partitioning the mesh and assigning each partition to a different node or thread. Such an execution model, with minor variations, is adopted, for example, in [Markall et al. 2013], [Logg et al. 2012], [AMCG 2010], [DeVito et al. 2011].

The time required to apply the numerical kernels is a major issue, since the equation domain needs to be discretized into an extremely large number of cells to obtain a satisfactory approximation of the PDE, possibly of the order of trillions, as in [Rossinelli et al. 2013]. For example, it has been well established that mesh resolution is critical in the accuracy of numerical weather forecasts. However, operational forecast centers have a strict time limit in which to produce a forecast - 60 minutes in the case of the UK Met Office. Producing efficient kernels has a direct scientific payoff in higher resolution, and therefore more accurate, forecasts. Computational cost is a dominant problem in computational science simulations, especially for those based on finite elements, which are the subject of this paper.

We address, in particular, the well-known problem of optimizing the local assembly phase of the finite element method [Russell and Kelly 2013; Olgaard and Wells 2010; Knepley and Terrel 2013; Kirby et al. 2005], which can be responsible for a significant fraction of the overall computation run-time, often in the range 30-60%. With respect to these studies, we propose a novel set of composable code transformations targeting, for the first time, cross-loop arithmetic intensity, with emphasis on instruction-level parallelism, redundant computation, and register locality. How such transformations generalize to domains other than finite element local assembly will also be discussed.

During the assembly phase, the solution of the PDE is approximated by executing a problem-specific kernel over all cells, or elements, in the discretized domain. In this work, we focus on relatively low order finite element methods, in which an assembly kernel's working set is usually small enough to fit the L1 cache. Low order methods are by no means exotic: they are employed in a wide variety of fields, including climate and ocean modeling, computational fluid dynamics, and structural mechanics. High order methods such as the spectral element method [Vos et al. 2010] commonly require different algorithms to solve PDEs and therefore are excluded from our study.

An assembly kernel is characterized by the presence of an affine, often non-perfect loop nest, in which individual loops are rather small: their trip count rarely exceeds 30, and may be as low as 3 for low order methods. In the innermost loop, a problem-specific, compute intensive expression evaluates a two dimensional array, representing the result of local assembly in an element of the discretized domain. With such a kernel structure, we focus on aspects like minimization of floating-point operations, register allocation and instruction-level parallelism, especially in the form of SIMD vectorization.

Achieving high-performance is non-trivial. The complexity of the mathematical expressions, often characterized by a large number of operations on constants and small matrices, makes it hard to determine a single or specific sequence of transformations that is successfully applicable to all problems. Loop trip counts are typically small and

can vary significantly, which further exacerbates the issue. A compiler-based approach is, therefore, the only reasonable option to obtain close-to-peak performance in a wide range of different local assembly kernels. Optimizations like padding, generalized loop-invariant code motion, vector-register tiling, and expression splitting, as well as their composition, are essential, but very limited is the support of state-of-the-art polyhedral and vendor compilers, if any. BLAS routines could theoretically be employed, although a fairly complicated control and data flow analysis would be required to automate identification and extraction of matrix-matrix multiplies. In addition, as detailed in Section 5.2.8, the small dimension of the matrices involved and the potential loss in data locality can limit or eliminate the performance gain of this approach.

In order to overcome the constraints of the available compilers and specialized linear algebra libraries, we have automated a set of generic and model-driven code transformations in COFFEE[1], a compiler for optimizing local assembly kernels. COFFEE is integrated with Firedrake [Firedrake contributors 2014], a system for solving PDEs through the finite element method based on the PyOP2 abstraction [Rathgeber et al. 2012; Markall et al. 2013]. All problems expressible with this framework are supported by COFFEE, including equations that can be found at the core of real-world simulations, such as those used in our performance evaluation. In evaluating our code transformations for a range of relevant problems, we vary two key parameters that impact solution accuracy and kernel cost: the polynomial order of the method (we investigate from $p = 1$ to $p = 4$) and the geometry of elements in the discretized domain (2D triangle, 3D tetrahedron, 3D prism). From the point of view of the generated code, these two parameters directly impact the size of both loop nests and mathematical expressions, as elaborated in Section 5.2.1.

Our experiments show that the original generated code for non-trivial assembly kernels, despite following state-of-the-art techniques, remains suboptimal in the context of modern multicore architectures. Our domain-aware cost-model-driven sequence of code transformations, aimed at improving SIMD vectorization and register data locality, can result in performance improvements up to $4.4\times$ over original kernels, and around 70% of the test cases obtain a speed up greater than $2\times$.

Summarizing, the contributions of this paper are

(1) An optimization strategy for finite element local assembly that exploits domain knowledge and goes beyond the limits of both vendor and research compilers.
(2) The design and implementation of a compiler that automates the proposed code transformations for any problems expressible in Firedrake.
(3) A systematic analysis using a suite of examples of real-world importance that is evidence of significant performance improvements on two Intel architectures, a Sandy Bridge CPU and the Xeon Phi.
(4) A full-application evaluation to demonstrate that the optimization strategy greatly impacts the whole finite element method.

Our contributions also include a theoretical study involving

(5) An analysis of the generality of the proposed code transformations and an investigation of their applicability to different computational domains.

The paper is organized as follows. In Section 2 we provide some background on local assembly, show code generated by Firedrake and emphasize the critical computational aspects. Section 3 describes the various code transformations, highlighting when and how domain knowledge has been exploited. The design and implementation of our

---

[1]COFFEE stands for COmpiler For FinitE Element local assembly.

```
Input: element matrix (2D array, initialized to 0), coordinates (array), coefficients (array, e.g. velocity)
Output: element matrix (2D array)
– Compute Jacobian from coordinates
– Define basis functions
– Compute element matrix in an affine loop nest
```

Fig. 1: Structure of a local assembly kernel

compiler is discussed in Section 4. Section 5 shows performance results. The generality of our optimization strategy and the applicability to other domains is discussed in Section 6. Related work is described in Section 7. Finally, Section 8 reviews our contributions in the light of our results, and identifies priorities for future work.

2. BACKGROUND AND MOTIVATING EXAMPLES

Local assembly is the computation of contributions of a specific cell in the discretized domain to the linear system which yields the PDE solution. The process consists of numerically evaluating problem-specific integrals to produce a matrix and a vector [Olgaard and Wells 2010; AMCG 2010], whose sizes depend on the order of the method. This operation is applied to all cells in the discretized domain. In this work we focus on local matrices, or "element matrices", which are more costly to compute than element vectors.

Given a finite element description of the input problem, expressed through the domain-specific Unified Form Language (UFL) [Alnæs et al. 2014], Firedrake employs the FEniCS form compiler (FFC) [Kirby and Logg 2006] to generate a C-code kernel implementing assembly using a numerical quadrature. This kernel can be applied to any element in the mesh, which follows from a mathematical property of the finite element method. The evaluation of a local matrix can be reduced to integration on a fixed "reference" element — a special element that does not belong to the domain — after a suitable change of coordinates. Firedrake triggers the compilation of an assembly kernel using an available vendor compiler, and manages its (parallel) execution over all elements in the mesh. As already explained, the subject of this paper is to enhance this execution model by adding an optimization stage prior to the generation of C code.

The structure of a local assembly kernel is shown in Figure 1. The inputs are a zero-initialized two dimensional array used to store the element matrix, the element's coordinates in the discretized domain, and coefficient fields, for instance indicating the values of velocity or pressure in the element. The output is the evaluated element matrix. The kernel body can be logically split into three parts:

(1) Calculation of the Jacobian matrix, its determinant and its inverse required for the aforementioned change of coordinates from the reference element to the one being computed.

Table I: Type and variable names used in the various listings to identify local assembly objects.

Object name	Type	Variable name(s)
Determinant of the Jacobian matrix	double	det
Inverse of the Jacobian matrix	double	K1, K2, ...
Coordinates	double**	coords
Fields	double**	w
Numerical integration weights	double[]	W
Basis functions (and derivatives)	double[][]	X, Y, X1, ...
Element matrix	double[][]	A

LISTING 1: Local assembly code generated by Firedrake for a Helmholtz problem on a 2D triangular mesh using Lagrange $p = 1$ elements.

```
void helmholtz(double A[3][3], double **coords) {
 // K, det = Compute Jacobian (coords)

 static const double W[3] = {...}
 static const double X_D10[3][3] = {{...}}
 static const double X_D01[3][3] = {{...}}

 for (int i = 0; i<3; i++)
  for (int j = 0; j<3; j++)
   for (int k = 0; k<3; k++)
    A[j][k] += ((Y[i][k]*Y[i][j]+
      +((K1*X_D10[i][k]+K3*X_D01[i][k])*(K1*X_D10[i][j]+K3*X_D01[i][j]))+
      +((K0*X_D10[i][k]+K2*X_D01[i][k])*(K0*X_D10[i][j]+K2*X_D01[i][j])))*
      *det*W[i]);
}
```

LISTING 2: Local assembly code generated by Firedrake for a Burgers problem on a 3D tetra-hedral mesh using Lagrange $p = 1$ elements.

```
void burgers(double A[12][12], double **coords, double **w) {
 // K, det = Compute Jacobian (coords)

 static const double W[5] = {...}
 static const double X1_D001[5][12] = {{...}}
 static const double X2_D001[5][12] = {{...}}
 //11 other basis functions definitions.
 ...
 for (int i = 0; i<5; i++) {
  double F0 = 0.0;
  //10 other declarations (F1, F2,...)
  ...
  for (int r = 0; r<12; r++) {
   F0 += (w[r][0]*X1_D100[i][r]);
   //10 analogous statements (F1, F2, ...)
   ...
  }
  for (int j = 0; j<12; j++)
   for (int k = 0; k<12; k++)
    A[j][k] += (..(K5*F9)+(K8*F10))*Y1[i][j])+
     +(((K0*X1_D100[i][k])+(K3*X1_D010[i][k])+(K6*X1_D001[i][k]))*Y2[i][j]))*F11+
     +(..((K2*X2_D100[i][k])+...+(K8*X2_D001[i][k]))*((K2*X2_D100[i][j])+...+(K8*X2_D001[i][j]))..)+
     + <roughly a hundred sum/muls go here>..)*
     *det*W[i]);
 }
}
```

---

(2) Definition of basis functions used, intuitively, to interpolate the contribution to the PDE solution over the element. The choice of basis functions is expressed in UFL directly by users. In the generated code, they are represented as global read-only two dimensional arrays (i.e., using static const in C) of double precision floats.
(3) Evaluation of the element matrix in an affine loop nest, in which the integration is performed.

Table I shows the variable names we will use in the upcoming code snippets to refer to the various kernel objects.

The actual complexity of a local assembly kernel depends on the finite element problem being solved. In simpler cases, the loop nest is perfect, has short trip counts (in the range 3–15), and the computation reduces to a summation of a few products involving basis functions. An example is provided in Listing 1, which shows the assembly kernel for a Helmholtz problem using Lagrange basis functions on 2D elements with polynomial order $p = 1$. In other scenarios, for instance when solving the Burgers equation, the number of arrays involved in the computation of the element matrix can be much larger. The assembly code is given in Listing 2 and contains 14 unique arrays that are accessed, where the same array can be referenced multiple times within the same expression. This may also require the evaluation of constants in outer loops (called F in the code) to act as scaling factors of arrays. Trip counts grow proportionally to the order of the method and arrays may be block-sparse. In addition to a larger number of operations, more complex cases like the Burgers equation are characterized by high register pressure.

The Helmholtz and Burgers equations exemplify a large class of problems and, as such, will constitute our benchmark problems, along with the Diffusion equation. We carefully motivate this choice in Section 5.2.1.

Despite the infinite variety of assembly kernels which Firedrake can generate, it is still possible to identify common domain-specific traits that can be exploited for effective code transformations and SIMD vectorization. These include: 1) memory accesses along the three loop dimensions are always unit stride; 2) the j and k loops are interchangeable, whereas interchanges involving the i loop require pre-computation of values (e.g. the F values in Burgers) and introduction of temporary arrays, as explained in Section 3; 3) depending on the problem being solved, the j and k loops could iterate over the same iteration space; 4) most of the sub-expressions on the right hand side of the element matrix computation depend on just two loops (either i-j or i-k). In Section 3 we show how to exploit these observations to define a set of systematic, composable optimizations.

3. CODE TRANSFORMATIONS

The code transformations presented in this section are applicable to all finite element problems that can be formulated in Firedrake. Their generality and the potential for applicability in other domains is also discussed in Section 6.

As already emphasized, the variations in the structure of mathematical expressions and in loop trip counts, although typically limited to the order of tens of iterations, render the optimization process challenging, requiring distinct sets of transformations to bring performance closest to the machine peak in different problems. For example, the Burgers problem in Listing 2, given the large number of arrays accessed, suffers from high register pressure, whereas the Helmholtz problem in Listing 1 does not; this intuitively suggests that the two problems require a different treatment, based on an in-depth analysis of both data and iteration spaces. Furthermore, domain-knowledge enables transformations that a general-purpose compiler could not apply, making the optimization space even larger. In this context, our goal is to understand the relationship between distinct code transformations, their impact on cross-loop arithmetic intensity, and to what extent their composability is effective in a class of problems and architectures.

3.1. Padding and Data Alignment

The absence of stencils renders the element matrix computation easily auto-vectorizable by a vendor compiler. Nevertheless, auto-vectorization is not efficient if data are not aligned to cache-line boundaries and if the length of the innermost loop is

not a multiple of the vector length `VL`, especially when the loops are small as in local assembly.

Data alignment is enforced in two steps. Firstly, all arrays are allocated to addresses that are multiples of `VL`. Then, two dimensional arrays are padded by rounding the number of columns to the nearest multiple of `VL`. For instance, assume the original size of a basis function array is $3{\times}3$ and $VL = 4$ (e.g. AVX processor, with 256-bit long vector registers and 64-bit double-precision floats). In this case, a padded version of the array will have size $3{\times}4$. The compiler is explicitly told about data alignment using suitable pragmas; for example, in the case of the Intel compiler, the annotation #pragma vector aligned is added over a loop (as shown in later figures) to inform that all of the memory accesses in the loop body will be properly aligned. This allows the compiler to issue aligned load and store instructions, which are notably faster than unaligned ones.

Padding of all two dimensional arrays involved in the evaluation of the element matrix also allows to safely round the loop trip count to the nearest multiple of `VL`. This avoids the introduction of a remainder (scalar) loop from the compiler, which would render vectorization less efficient. These extra iterations only write to the padded region of the element matrix, and therefore have no side effects on the final result.

3.2. Generalized Loop-invariant Code Motion

From the inspection of the codes in Listings 1 and 2, it can be noticed that the computation of A involves evaluating many sub-expressions which only depend on two iteration variables. Since symbols in most of these sub-expressions are read-only variables, there is ample space for loop-invariant code motion. Vendor compilers apply this technique, although not in the systematic way we need for our assembly kernels. We want to overcome two deficiencies that both Intel and GNU compilers exhibit. First, they only identify sub-expressions that are invariant with respect to the innermost loop. This is an issue for sub-expressions depending on `i-k`, which are not automatically lifted in the loop order `ijk`. Second, the hoisted code is scalar and therefore not subjected to auto-vectorization.

We work around these limitations with source-level loop-invariant code motion. In particular, we pre-compute all values that an invariant sub-expression assumes along its fastest varying dimension. This is implemented by introducing a temporary array per invariant sub-expression and by adding a new loop to the nest. At the price of extra memory for storing temporaries, the gain is that lifted terms can be auto-vectorized as part of an inner loop. Given the short trip counts of our loops, it is important to achieve auto-vectorization of hoisted terms in order to minimize the percentage of scalar instructions, which could otherwise be significant. It is also worth noting that, in some problems (e.g. Helmholtz), invariant sub-expressions along `j` are identical to those along `k`, and both loops iterate over the same iteration space, as anticipated in Section 2. In these cases, we safely avoid redundant pre-computation.

Listing 3 shows the Helmholtz assembly code after the application of loop-invariant code motion, padding, and data alignment.

3.3. Model-driven Vector-register Tiling

One notable problem of assembly kernels concerns register allocation and register locality. The critical situation occurs when loop trip counts and the variables accessed are such that the vector-register pressure is high. Since the kernel's working set fits the L1 cache, it is particularly important to optimize register management. Standard optimizations, such as loop interchange, unroll, and unroll-and-jam, can be employed to deal with this problem. In COFFEE, these optimizations are supported either by means of explicit code transformations (interchange, unroll-and-jam) or indirectly by

LISTING 3: Local assembly code for the Helmholtz problem in Listing 1 after application of padding, data alignment, and *licm*, for an AVX architecture. In this example, sub-expressions invariant to j are identical to those invariant to k, so they can be precomputed once in the r loop.

```
void helmholtz(double A[3][4], double **coords) {
 #define ALIGN __attribute__((aligned(32)))
 // K, det = Compute Jacobian (coords)

 static const double W[3] ALIGN = {...}
 static const double X_D10[3][4] ALIGN = {{...}}
 static const double X_D01[3][4] ALIGN = {{...}}

 for (int i = 0; i<3; i++) {
  double LI_0[4] ALIGN;
  double LI_1[4] ALIGN;
  for (int r = 0; r<4; r++) {
   LI_0[r] = ((K1*X_D10[i][r])+(K3*X_D01[i][r]));
   LI_1[r] = ((K0*X_D10[i][r])+(K2*X_D01[i][r]));
  }
  for (int j = 0; j<3; j++)
   #pragma vector aligned
   for (int k = 0; k<4; k++)
    A[j][k] += (Y[i][k]*Y[i][j]+LI_0[k]*LI_0[j]+LI_1[k]*LI_1[j])*det*W[i]);
 }
}
```

delegation to the compiler through standard pragmas (unroll). Tiling at the level of vector registers is an additional feature of COFFEE. Based on the observation that the evaluation of the element matrix can be reduced to a summation of outer products along the j and k dimensions, a model-driven vector-register tiling strategy can be implemented. If we consider the code snippet in Listing 3 and we ignore the presence of the operation det*W3[i], the computation of the element matrix is abstractly expressible as

$$A_{jk} = \sum_{\substack{x \in B' \subseteq B \\ y \in B'' \subseteq B}} x_j \cdot y_k \qquad j, k = 0, ..., 2 \tag{1}$$

where B is the set of all basis functions (or temporary variables, e.g., LI_0) accessed in the kernel, whereas B' and B'' are generic problem-dependent subsets. Regardless of the specific input problem, by abstracting from the presence of all variables independent of both j and k, the element matrix computation is always reducible to this form. Figure 2 illustrates how we can evaluate 16 entries ($j, k = 0, ..., 3$) of the element matrix using just 2 vector registers, which represent a 4×4 tile, assuming $|B'| = |B''| = 1$. Values in a register are shuffled each time a product is performed. Standard compiler auto-vectorization for both GNU and Intel compilers, instead, executes 4 broadcast operations (i.e., "splat" of a value over all of the register locations) along the outer dimension to perform the calculation. In addition to incurring a larger number of cache accesses, it needs to keep between $f = 1$ and $f = 3$ extra registers to perform the same 16 evaluations when unroll-and-jam is used, with f being the unroll-and-jam factor.

The storage layout of A, however, is incorrect after the application of this outer-product-based vectorization (*op-vect*, in the following). It can be efficiently restored with a sequence of vector shuffles following the pattern highlighted in Figure 3, executed once outside of the ijk loop nest. The generated pseudo-code for the simple Helmholtz problem when using *op-vect* is shown in Figure 4.
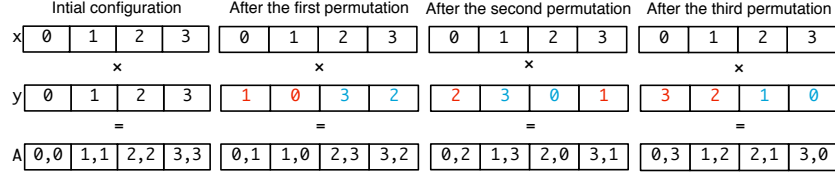
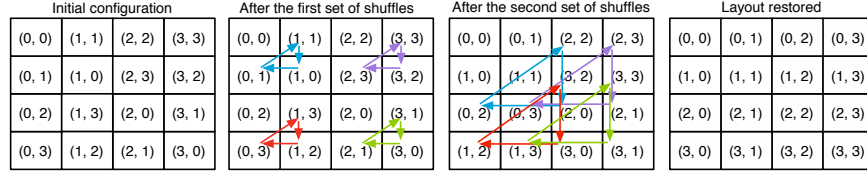Fig. 2: Outer-product vectorization by permuting values in a vector register.

Fig. 3: Restoring the storage layout after *op-vect*. The figure shows how 4×4 elements in the top-left block of the element matrix A can be moved to their correct positions. Each rotation, represented by a group of three same-colored arrows, is implemented by a single shuffle intrinsic.

3.4. Expression Splitting

In complex kernels, like Burgers in Listing 2, and on certain architectures, achieving effective register allocation can be challenging. If the number of variables independent of the innermost-loop dimension is close to or greater than the number of available CPU registers, poor register reuse is likely. This usually happens when the number of basis function arrays, temporaries introduced by generalized loop-invariant code motion, and problem constants is large. For example, applying loop-invariant code motion to Burgers on a 3D mesh requires 24 temporaries for the ijk loop order. This can make hoisting of the invariant loads out of the k loop inefficient on architectures with a relatively low number of registers. One potential solution to this problem consists of suitably "splitting" the computation of the element matrix A into multiple sub-expressions; an example, for the Helmholtz problem, is given in Listing 5. The transformation can be regarded as a special case of classic loop fission, in which associativity of the sum is exploited to distribute the expression across multiple loops. To the best of our knowledge, expression splitting is not supported by available compilers.

Splitting an expression has, however, several drawbacks. Firstly, it increases the number of accesses to A proportionally to the "split factor", which is the number of sub-expressions produced. Also, depending on how the split is executed, it can lead to redundant computation. For example, the number of times the product $det * W3[i]$ is performed is proportional to the number of sub-expressions, as shown in the code snippet. Further, it increases loop overhead, for example through additional branch instructions. Finally, it might affect register locality: for instance, the same array could be accessed in different sub-expressions, requiring a proportional number of loads be performed. This is not the case for the Helmholtz example. Nevertheless, as shown in Section 5, the performance gain from improved register reuse along inner dimensions can still be greater, especially if the split factor and the splitting itself use heuristics to minimize the aforementioned issues.

LISTING 4: Local assembly code generated by Firedrake for the Helmholtz problem after application of *op-vect* on top of the optimizations shown in Listing 3. In this example, the unroll-and-jam factor is 1.

```
void helmholtz(double A[4][4], double **coords) {
 // K, det = Compute Jacobian (coords)
 // Declaration of basis function matrices

 for (int i = 0; i<3; i++) {
  // Do generalized loop-invariant code motion
  for (int j = 0; j<4; j+=4)
   for (int k = 0; k<4; k+=4) {
    // load and set intrinsics
    // Compute A[0,0], A[1,1], A[2,2], A[3,3]
    // One permute_pd intrinsic per k-loop load
    // Compute A[0,1], A[1,0], A[2,3], A[3,2]
    // One permute2f128_pd intrinsic per k-loop load
    // ...
   }
  // Remainder loop (from j = 4 to j = 6)
 }
 // Restore the storage layout:
 for (int j = 0; j<4; j+=4) {
  __m256d r0, r1, r2, r3, r4, r5, r6, r7;
  for (int k = 0; k<4; k+=4) {
   r0 = _mm256_load_pd (&A[j+0][k]);
   // Load A[j+1][k], A[j+2][k], A[j+3][k]
   r4 = _mm256_unpackhi_pd (r1, r0);
   r5 = _mm256_unpacklo_pd (r0, r1);
   r6 = _mm256_unpackhi_pd (r2, r3);
   r7 = _mm256_unpacklo_pd (r3, r2);
   r0 = _mm256_permute2f128_pd (r5, r7, 32);
   r1 = _mm256_permute2f128_pd (r4, r6, 32);
   r2 = _mm256_permute2f128_pd (r7, r5, 49);
   r3 = _mm256_permute2f128_pd (r6, r4, 49);
   _mm256_store_pd (&A[j+0][k], r0);
   // Store A[j+1][k], A[j+2][k], A[j+3][k]
  }
 }
}
```

LISTING 5: Local assembly code generated by Firedrake for the Helmholtz problem in which *split* has been applied on top of the optimizations shown in Listing 3. In this example, the split factor is 2.

```
void helmholtz(double A[3][4], double **coords) {
 // Same code as in Listing 3 up to the j loop
  for (int j = 0; j<3; j++)
   #pragma vector aligned
   for (int k = 0; k<4; k++)
    A[j][k] += (Y[i][k]*Y[i][j]+LI_0[k]*LI_0[j])*det*W3[i];
  for (int j = 0; j<3; j++)
   #pragma vector aligned
   for (int k = 0; k<4; k++)
    A[j][k] += LI_1[k]*LI_1[j]*det*W3[i];
}
```

Table II summarizes the code transformations described so far. Given that many of these transformations depend on some parameters (e.g. tile size), we need a mechanism to prune such a large optimization space. This aspect is treated in Section 4.

Table II: Overview of code transformations for Firedrake-generated assembly kernels.

Name (Abbreviation)	Parameter
Generalized loop-invariant code motion (*licm*)	
Padding	
Data Alignment	
Loop interchange	loops
Loop unrolling	unroll factor
Outer-product vectorization (*op-vect*)	tile size
Expression splitting (*split*)	split point, split factor

4. OVERVIEW OF COFFEE

Firedrake users employ the Unified Form Language to express problems in a notation resembling mathematical equations. At run-time, the high-level specification is translated by a modified version of the FEniCS Form Compiler (FFC) [Kirby and Logg 2006] into an abstract syntax tree (AST) representation of one or more finite element assembly kernels. ASTs are then passed to COFFEE to apply the transformations described in Section 3. The output of COFFEE, C code, is eventually provided to PyOP2 [Rathgeber et al. 2012; Markall et al. 2013], where just-in-time compilation and execution over the discretized domain take place. The flow is summarized in Figure 4.

Because of the large number of parametric transformations, COFFEE needs a mechanism to select the most suitable optimization strategy for a given problem. Autotuning might be used, although it would significantly increase the run-time overhead, since the generation of ASTs occurs at run-time as soon as problem-specific data are available. Our optimization strategy, based on heuristics and a simple cost model, is described in the following, along with an overview of the compiler.

The compiler structure is outlined in Figure 5. Initially the AST is inspected, looking for the presence of iteration spaces and domain-specific information provided by the higher layer. If the kernel lacks an iteration space, then so-called inter-kernel vectorization, in which the outer, non-affine loop over mesh elements is vectorized, can be applied. This feature, currently under development, has been shown to be useful in several finite volume applications [Reguly et al. 2007]. Subsequently, an ordered sequence of optimization steps are executed. Application of *licm* must precede padding and data alignment, due to the introduction of temporary arrays. Based on a cost model, loop interchange, *split*, and *op-vect* may be introduced. Their implementation is based on analysis and transformation of the kernel's AST. When *op-vect* is selected, the compiler

Fig. 4: High-level view of Firedrake. COFFEE is at the core, receiving ASTs from a modified version of the FEniCS Form compiler and producing optimized C code kernels.

```
Input: ast (kernel abstract syntax tree), wrapper (function invoking the kernel),
       isa (SIMD Instruction Set Architecture)
Output: assembly code (C string)
// Analyze ast and build optimization plan
it_space = analyze(ast)
if not it_space
  ast.apply_inter_kernel_vectorization(wrapper, isa)
  return wrapper + ast.from_ast_to_c()
plan = cost_model(it_space.n_inner_arrays, isa.n_regs)
// Optimize ast based on plan
ast.licm()
ast.padding()
ast.align_data()
if plan.permute
  ast.permute_assembly_loops()
if plan.split_factor
  ast.split(plan.split_factor)
if plan.uaj_factor
  uaj = MIN(plan.uaj_factor, it_space.j.size/isa.vf)
  ast.op_vect(uaj)
return wrapper + ast.from_ast_to_c()
```

Fig. 5: Outline of the COFFEE architecture.

outputs AVX or AVX-512 intrinsics code. Any possible corner cases are handled: for example, if *op-vect* is to be applied, but the size of the iteration space is not a multiple of the vector length, then a remainder loop, amenable to auto-vectorization, is inserted.

Loop interchange. All loops are interchangeable, provided that temporaries are introduced if the nest is not perfect. For the employed storage layout, the loop permutations ijk and ikj are likely to maximize performance. Conceptually, this is motivated by the fact that if the i loop were in an inner position, then a significantly higher number of load instructions would be required at every iteration. We tested this hypothesis in manually crafted kernels. We found that the performance loss is greater than the gain due to the possibility of accumulating increments in a register, rather than memory, along the i loop. The choice between ijk and ikj depends on the number of load instructions that can be hoisted out of the innermost dimension. Our compiler chooses as outermost the loop along which the number of invariant loads is smaller so that more registers remain available to carry out the computation of the element matrix.

Loop unrolling. Loop unroll (or unroll-and-jam of outer loops) is fundamental to the exposure of instruction-level parallelism, and tuning unroll factors is particularly important.

We first observe that manual full (or extensive) unrolling is unlikely to be effective. The ijk loop nest would need to be small enough such that the unrolled instructions do not exceed the instruction cache, which is rarely the case: it is true that in a local assembly kernel the minimum size of the ijk loop nest is $3\times3\times3$ (triangular mesh and polynomial order 1), but this increases rapidly with the polynomial order of the method and the discretization employed (e.g. tetrahedral meshes imply larger loop nests than triangular ones), so sizes greater than $10\times10\times10$, for which extensive unrolling would already be harmful, are in practice very common. In addition, manual unrolling is dangerous because it may compromise compiler auto-vectorization by either removing loops (most compilers search for vectorizable loops) or losing spatial locality within a vector register.

By comparison with implementations characterized by manually-unrolled loops, we noticed that recent versions of compilers like GNU's and Intel's estimate close-to-optimal unroll factors when the loops are affine and their bounds are relatively small and known at compile-time, which is the case of our kernels. Our choice, therefore, is

```
1   Input: n_outer_arrays, n_inner_arrays, n_consts, n_regs
2   Output: uaj_factor, split_factor
3   n_outer_regs = n_regs / 2
4   split_factor = 0
5   // Compute spltting factor
6   while n_outer_arrays > n_outer_regs
7     n_outer_arrays = n_outer_arrays / 2
8     split_factor = split_factor + 1
9   // Compute unroll-and-jam factor for op-vect
10  n_regs_avail = n_regs - (n_outer_arrays + n_consts)
11  uaj_factor = n_reg_avail / n_inner_arrays
12  // Estimate the benefit of permuting loops
13  permute = n_outer_arrays > n_inner_arrays
14  return <permute, split_factor, uaj_factor>
```

Fig. 6: The cost model is employed by the compiler to estimate the most suitable unroll-and-jam (when *op-vect* is used) and split factors, avoiding the overhead of auto-tuning.

to leave the backend compiler in charge of selecting unroll factors. This also simplifies the COFFEE's cost model, described next. The only situation in which we explicitly unroll-and-jam a loop is when *op-vect* is used, since the transformed code prevents the Intel compiler from applying this optimization, even if specific pragmas are added.

Cost model. The cost model is shown in Figure 6. It takes into account the number of available logical vector registers, n_regs, and the number of unique variables accessed: n_consts counts variables independent of both j and k loops and temporary registers, n_outer_arrays counts j-dependent variables, and n_inner_arrays counts k-dependent variables, assuming the ijk loop order. These values are used to estimate unroll-and-jam and split factors for *op-vect* and *split*. If a factor is 0, then the corresponding transformation is not applied. The *split* transformation is triggered whenever the number of hoistable terms is larger than the available registers along the outer dimension (lines 3-8), which is approximated as half of the total (line 3). A split factor of n means that the assembly expression should be "cut" into n sub-expressions. Depending on the structure of the assembly expression, each sub-expression might end up accessing a different number of arrays; the cost model is simplified by assuming that all sub-expressions are of the same size. The unroll-and-jam factor for the *op-vect* transformation is determined as a function of the available logical registers, i.e., those not used for storing hoisted terms (line 9-11). Finally, the profitability of loop interchange is evaluated (line 13).

5. PERFORMANCE EVALUATION

5.1. Experimental Setup

Experiments were run on a single core of two Intel architectures, a Sandy Bridge (I7-2600 CPU, running at 3.4GHz, 32KB L1 cache and 256KB L2 cache) and a Xeon Phi (5110P, running at 1.05Ghz in native mode, 32KB L1 cache and 512KB L2 cache). We have chosen these two architectures because of the differences in the number of logical registers and SIMD lanes (16 256-bit registers in the Sandy Bridge, and 32 512-bit registers in the Xeon Phi), which can impact the optimization strategy. The icc 13.1 compiler was used. On the Sandy Bridge, the compilation flags used were -O2 and -xAVX for auto-vectorization. On the Xeon Phi, optimization level -O3 was used. Other optimization levels performed, in general, slightly worse.

We present two studies. Firstly, in Section 5.2, we analyze the impact of the proposed code transformations, and their interplay, in three real-world representative equations. We quantify the speed ups achievable at the level of the local assembly kernel, i.e. by excluding from the measurements the other sections of the computation.

Then, in Section 5.3, we provide a full-application investigation. Here, we use another equation (so as to bring the total number of examined problems to four) to demonstrate that COFFEE's optimizations actually allow a significant reduction in the overall computation run-time to be achieved, which practically motivates our research.

5.2. In-depth Performance Analysis of the Code Transformations and their Interplay

5.2.1. Choice and Properties of the Benchmarks. Our code transformations were evaluated in three real-world problems based on the following PDEs

(1) Helmholtz
(2) Advection-Diffusion
(3) Burgers

The three chosen benchmarks are *real-life kernels* and comprise the core differential operators in some of the most frequently encountered finite element problems in scientific computing. This is of crucial importance because distinct problems, possibly arising in completely different fields, may employ (subsets of) the same differential operators of our benchmarks, which implies similarities and redundant patterns in the generated code. Consequently, the proposed code transformations have a domain of applicability that goes far beyond that of the three analyzed equations.

The Helmholtz and Diffusion kernels are archetypal second order elliptic operators. They are complete and unsimplified examples of the operators occurring for diffusion and viscosity in fluids, and for imposing pressure in compressible fluids. As such, they are both extensively used in climate and ocean modeling. Very similar operators, for which the same optimisations are expected to be equally effective, apply to elasticity problems, which are at the base of computational structural mechanics. The Burgers kernel is a typical example of a first order hyperbolic conservation law, which occurs in real applications whenever a quantity is transported by a fluid (the momentum itself, in our case). We chose this particular kernel since it applies to a vector-valued quantity, while the elliptic operators apply to scalar quantities; this impacts the generated code, as explained next. In this way, the operators we have selected are characteristic of both the second and first order operators that dominate in fluids and solids simulations, and a wide variety on local assembly codes can be tested.

The benchmarks were written in UFL (code available at [Luporini 2014a]) and executed over real unstructured meshes through Firedrake. The Helmholtz code has already been shown in Listing 1. For Advection-Diffusion, the Diffusion equation, which uses the same differential operators as Helmholtz, is considered. In the Diffusion kernel code, the main differences with respect to Helmholtz are the absence of the Y array and the presence of a few more constants for computing the element matrix. Burgers is a non-linear problem employing differential operators different from those of Helmholtz and relying on vector-valued quantities, which has a major impact on the generated assembly code (see Listing 2), where a larger number of basis function arrays ($X1$, $X2$, ...) and constants ($F0$, $F1$, ..., $K0$, $K1$, ...) are generated.

These problems were studied varying both the shape of mesh elements and the polynomial order p of the method, whereas the element family, Lagrange, is fixed. As might be expected, the larger the element shape and p, the larger the iteration space. Triangles, tetrahedron, and prisms were tested as element shape. For instance, in the case of Helmholtz with $p = 1$, the size of the j and k loops for the three element shapes is, respectively, 3, 4, and 6. Moving to bigger shapes has the effect of increasing the number of basis function arrays, since, intuitively, the behaviour of the equation has now to be approximated also along a third axis. On the other hand, the polynomial order affects only the problem size (the three loops i, j, and k, and, as a consequence, the size of X and Y arrays). A range of polynomial orders from $p = 1$ to $p = 4$ were tested;

Table III: Performance improvement due to generalized loop-invariant code motion, for different element shapes (triangle, tetrahedron, prism) and polynomial orders ($p \in [1, 4]$), over the original non-optimized code, for the Helmholtz, Diffusion and Burgers problems.

problem	shape	Sandy Bridge				Xeon Phi			
		p1	p2	p3	p4	p1	p2	p3	p4
Helmholtz	triangle	1.05	1.46	1.68	1.67	1.49	1.06	1.05	1.17
Helmholtz	tetrahedron	1.36	2.10	2.64	2.27	1.28	1.29	2.05	1.73
Helmholtz	prism	2.16	2.28	2.45	2.06	1.04	2.26	1.93	1.64
Diffusion	triangle	1.09	1.68	1.97	1.64	1.07	1.06	1.18	1.16
Diffusion	tetrahedron	1.30	2.20	3.12	2.60	1.00	1.38	2.02	1.74
Diffusion	prism	2.15	1.82	2.71	2.32	1.11	2.16	1.85	2.83
Burgers	triangle	1.53	1.81	2.68	2.46	1.21	1.42	2.34	2.97
Burgers	tetrahedron	1.61	2.24	1.69	1.59	1.01	2.55	0.98	1.21
Burgers	prism	2.11	2.20	1.66	1.32	1.39	1.56	1.18	1.04

higher polynomial orders are excluded from the study because of current Firedrake limitations. In all these cases, the size of the element matrix rarely exceeds 30×30, with a peak of 105×105 in Burgers with prisms and $p = 4$.

5.2.2. Loop interchange. In the following, only results for the loop order ijk are shown. For the considerations exposed in Section 4, loop interchanges having an inner loop along i caused slow downs; also, interchanging j and k loops while keeping i as outer-most loop did not provide any benefits.

5.2.3. Impact of Generalized Loop-invariant Code Motion. Table III illustrates the performance improvement obtained when *licm* is applied. In general, the speed ups are notable. The main reasons were anticipated in Section 3.2: in the original code, 1) sub-expressions invariant to outer loops are not automatically hoisted, while 2) sub-expressions invariant to the innermost loop are hoisted, but their execution is not auto-vectorized. These observations come from inspection of assembly code generated by the compiler.

The gain tends to grow with the computational cost of the kernels: bigger loop nests (i.e., larger element shapes and polynomial orders) usually benefit from the reduction in redundant computation, even though extra memory for the temporary arrays is required. Some discrepancies to this trend are due to a less effective auto-vectorization. For instance, on the Sandy Bridge, the improvement at $p = 3$ is larger than that at $p = 4$ because, in the latter case, the size of the innermost loop is not a multiple of the vector length, and a reminder scalar loop is introduced at compile time. Since the loop nest is small, the cost of executing the extra scalar iterations can have a significant impact. The reminder loop overhead is more pronounced on the Xeon Phi, where the vector length is twice as big, which leads to proportionally larger scalar reminder loops.

5.2.4. Impact of Padding and Data Alignment. Table IV shows the cumulative impact of *licm*, data alignment, and padding over the original code. In the following, this version of the code is referred to as *licm-ap*. Padding, which avoids the introduction of a reminder loop as described in Section 5.2.3, as well as data alignment, enhance the quality of auto-vectorization. Occasionally the run-time of *licm-ap* is close to that of *licm*, since the non-padded element matrix size is already a multiple of the vector length. Rarely *licm-ap* is slower than *licm* (e.g. in Burgers $p = 3$ on the Sandy Bridge). One possible explanation is that the number of aligned temporaries introduced by *licm* is so large to induce cache associativity conflicts.

Table IV: Performance improvement due to generalized loop-invariant code motion, data alignment, and padding, for different element shapes (triangle, tetrahedron, prism) and polynomial orders ($p \in [1,4]$), over the original non-optimized code, for the Helmholtz, Diffusion and Burgers problems.

		Sandy Bridge				Xeon Phi			
problem	shape	p1	p2	p3	p4	p1	p2	p3	p4
Helmholtz	triangle	1.32	1.88	2.87	4.13	1.50	2.41	1.30	1.96
Helmholtz	tetrahedron	1.35	3.32	2.66	3.27	1.41	1.50	2.79	2.81
Helmholtz	prism	2.63	2.74	2.43	2.75	2.38	2.47	2.15	1.71
Diffusion	triangle	1.38	1.99	3.07	4.28	1.08	1.88	1.20	1.97
Diffusion	tetrahedron	1.41	3.70	3.18	3.82	1.05	1.51	2.76	3.00
Diffusion	prism	2.55	3.13	2.73	2.69	2.41	2.52	2.05	2.48
Burgers	triangle	1.56	2.28	2.61	2.77	2.84	2.26	3.96	4.27
Burgers	tetrahedron	1.61	2.10	1.60	1.78	1.48	3.83	1.55	1.29
Burgers	prism	2.19	2.32	1.64	1.42	2.18	2.82	1.24	1.25

5.2.5. Impact of Vector-register Tiling. In this section, we evaluate the impact of vector-register tiling. We compare two versions: the baseline, *licm-ap*; and vector-register tiling on top of *licm-ap*, which in the following is referred to simply as *op-vect*.

Figures 7 and 8 illustrate the speed up achieved by *op-vect* over *licm-ap* in the Helmoltz and Diffusion kernels, respectively. As explained in Section 4, the *op-vect* version requires the unroll-and-jam factor to be explicitly set. To distinguish between the two ways this parameter was determined, for each problem instance (equation, element shape, polynomial order) we report two bars: one shows the best speed-up obtained after all feasible unroll-and-jam factors were tried; the other shows the speed up when the unroll-and-jam factor was retrieved via the cost model. In a plot legend, cost model bars are suffixed with "CM".

It is worth noticing that, in most cases, the cost model successfully determines how to transform a kernel to maximize its performance. This is chiefly because assembly kernels fit the L1 cache, so, within a certain degree of confidence, it is possible to predict how to obtain a fast implementation by simply reasoning on the register pressure. For each problem, the cost model stated to use the default loop permutation, to apply a particular unroll-and-jam factor, and not to perform expression splitting, which, as explained in Section 5.2.6, only deteriorates performance in Helmholtz and Diffusion.

The rationale behind these results is that the effect of *op-vect* is significant in problems in which the assembly loop nest is relatively big. When the loops are short, since the number of arrays accessed at every loop iteration is rather small (between 4 and 8 temporaries, plus the element matrix itself), there is no need for vector-register tiling; extensive unrolling is sufficient to improve register re-use and, therefore, to maximize the performance. However, as the iteration space becomes larger, *op-vect* leads to improvements up to $1.4\times$ on the Sandy Bridge (Diffusion, prismatic mesh, $p = 4$ - increasing the overall speed up from $2.69\times$ to $3.87\times$), and up to $1.4\times$ on the Xeon Phi (Helmholtz, tetrahedral mesh, $p = 3$ - bringing the overall speed up from $1.71\times$ to $2.42\times$).

Using the Intel Architecture Code Analyzer tool [Intel Corporation 2012] on the Sandy Bridge, we confirmed that speed ups are a consequence of increased register re-use. In Helmholtz $p = 4$, for example, the tool showed that when using *op-vect* the number of clock cycles to execute one iteration of the j loop decreases by roughly 17%, and that this is a result of the relieved pressure on both of the data (cache) ports available in the core.

On the Sandy Bridge, we have also measured the performance of individual kernels in terms of floating-point operations per second. The theoretical peak on a single core, with the Intel Turbo Boost technology activated, is 30.4 GFlop/s. In the case of Diffu-
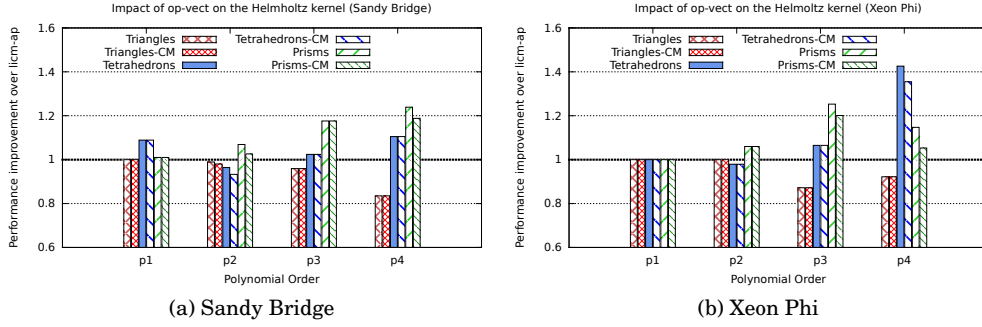
Fig. 7: Performance improvement over *licm-ap* obtained by *op-vect* in the Helmholtz kernel. Bars suffixed with "CM" indicate that the cost model was used to transform the kernel.
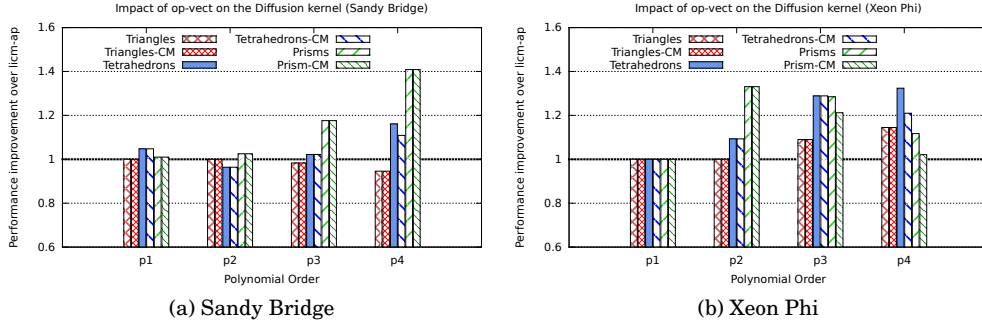

Fig. 8: Performance improvement over *licm-ap* obtained by *op-vect* in the Diffusion kernel. Bars suffixed with "CM" indicate that the cost model was used to transform the kernel.

sion using a prismatic mesh and $p = 4$, we achieved a maximum of 21.9 GFlop/s with *op-vect* enabled, whereas 16.4 GFlop/s was obtained when only *licm-ap* is used. This result is in line with the expectations: analysis of assembly code showed that, in the jk loop nest, which in this problem represents the bulk of the computation, 73% of instructions are actually floating-point operations.

Application of *op-vect* to the Burgers problem induces significant slow downs due to the large number of temporary arrays that need to be tiled, which exceeds the available logical registers on the underlying architecture. Expression splitting can be used in combination with *op-vect* to alleviate this issue; this is discussed in the next section.

5.2.6. Impact of Expression Splitting. Expression splitting relieves the register pressure when the element matrix evaluation needs to read from a large number of basis function arrays. As detailed in Section 3.4, in the price to pay for this optimazion, there are an increased number of accesses to the element matrix and, potentially, redundant computation. Similarly to the analysis of vector-register tiling, we compare two versions: the baseline, *licm-ap*; and expression splitting on top of *licm-ap*, which, for simplicity, in the following is referred to as *split*.
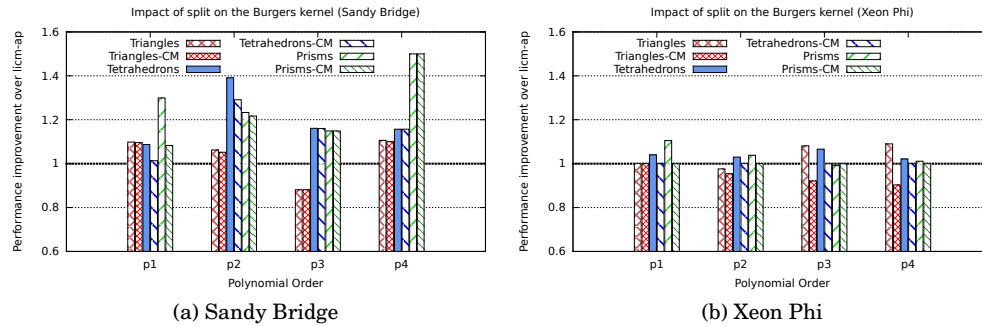
Fig. 9: Performance improvement over *licm-ap* obtained by *split* in the Burgers kernel. Bars suffixed with "CM" indicate that the cost model was used to transform the kernel.

For the Helmholtz and Diffusion kernels, in which only between 4 and 8 temporaries are read at every loop iteration, split tends to slow down the computation, because of the aforementioned drawbacks. Slow downs up to $1.4\times$ and up to $1.6\times$ were observed, respectively, on the Sandy Bridge and the Xeon Phi. Note that the cost model prevents the adoption of the transformation: the while statement in Figure 6 is indeed never entered.

In the Burgers kernels, between 12 and 24 temporaries are accessed at every loop iteration, so *split* plays a key role on the Sandy Bridge, where the number of available logical registers is only 16. Figure 9 shows the performance improvement achieved by *split* over *licm-ap*. In almost all cases, a split factor of 1, meaning that the original expression was divided into two parts, ensured close-to-peak perforance. The transformation negligibly affected register locality, so speed ups up to $1.5\times$ were observed. For instance, on the Sandy Bridge, when $p = 4$ and a prismatic mesh is employed, the overall performance improvement (i.e., the one over the original code) increases from $1.44\times$ to $2.11\times$. On the Xeon Phi, the impact of *split* is only marginal, since register spilling is limited by the presence of 32 logical vector units.

On the Sandy Bridge, the performance of the Burgers kernel on a prismatic mesh was 20.0 GFlop/s from $p = 1$ to $p = 3$, while it was 21.3 GFlop/s in the case of $p = 4$. These values are notably close to the peak performance of 30.4 GFlop/s. Disabling *split* makes the performance drop to 17.0 GFlop/s for $p = 1, 2$, 18.2 GFlop/s for $p = 3$, and 14.3 GFlop/s for $p = 4$. These values are in line with the speedups shown in Figure 9.

The *split* transformation was also tried in combination with *op-vect* (*split-op-vect*), although the cost model prevents its adoption on both platforms. Despite improvements up to $1.22\times$, *split-op-vect* never outperforms *split*. This is motivated by two factors: for small split factors, such as 1 and 2, the data space to be tiled is still too big, and register spilling affects run-time; for higher ones, sub-expressions become so small that, as explained in Section 5.2.5, extensive unrolling already allows to achieve a certain degree of register re-use.

5.2.7. Comparison with FEniCS Form Compiler's built-in Optimizations. We have modified the FEniCS Form Compiler (FFC) to return an abstract syntax tree representation of a local assembly kernel, rather than plain C++ code, so as to enable code transformations in COFFEE. Besides Firedrake, FFC is used in the FEniCS project [Logg et al. 2012]. In FEniCS, FFC can apply its own model-driven optimizations to local assembly kernels [Olgaard and Wells 2010], which mainly consist of loop-invariant code motion and

elimination, at code generation time, of floating point operations involving zero-valued entries in basis function arrays.

The FEniCS Form Compiler's loop-invariant code motion is different from COF-FEE's. It is based on expansion of arithmetic operations, for example applying distributivity and associativity to products and sums at code generation time, to identify terms that are invariant of the whole loop nest. Depending on the way expansion is performed, operation count may not decrease significantly.

Elimination of zero-valued terms, which are the result of using vector-valued quantities in the finite element problem, has the effect of introducing indirection arrays in the generated code. This kind of optimization is currently under development in COFFEE, although it will differ from FEniCS' by avoiding non-contiguous memory accesses, which would otherwise affect vectorization, at the price of removing fewer zero-valued contributions.

Table V summarizes the performance achieved by COFFEE over the *fastest* FEniCS (FFC) implementation on the Sandy Bridge for the Burgers, Helmholtz and Diffusion kernels. Burgers' slow downs occur in presence of a small iteration space (triangular mesh, $p \in [1, 2]$; tetrahedral mesh, $p \in [1, 2]$; prismatic mesh, $p = 1$). The result shown represents the worst slow down, which was obtained with a triangular mesh and $p = 1$. This is a result of removing zero-valued entries in FEniCS' basis function arrays: some operations are avoided, but indirection arrays prevent auto-vectorization, which significantly impacts performance as soon as the element matrix becomes bigger than 12×12. However, with the forthcoming zero-removal optimization in COF-FEE, we expect to outperform FEniCS in all problems. In the cases of Helmholtz and Diffusion, the minimum improvements are, respectively, $1.10 \times$ and $1.18 \times$ (2D mesh, $p = 1$), which tend to increase with polynomial order and element shape up to the values illustrated in the table.

Table V: Performance comparison between FEniCS and COFFEE on the Sandy Bridge.

Problem	Max slow down	Max speed up
Helmholtz	-	$4.14\times$
Diffusion	-	$4.28\times$
Burgers	$2.24\times$	$1.61\times$

5.2.8. Comparison with hand-made BLAS-based implementations. For the Helmholtz problem on a tetrahedral mesh, manual implementations based on `Intel MKL BLAS` were tested on the Sandy Bridge. This particular kernel can be easily reduced to a sequence of four matrix-matrix multiplies that can be computed via calls to BLAS `dgemm`. In the case of $p = 4$, where the element matrix is of size 35×35, the computation was almost twice slower than the case in which *licm-ap* was used, with the slow down being even worse for smaller problem sizes. These experiments suggest that the question regarding to what extent linear algebra libraries can improve performance cannot be trivially answered. This is due to a combination of issues: the potential loss in data locality, as exposed in Section 3.4, the actual effectiveness of these libraries when the arrays are relatively small, and the problem inherent to assembly kernels concerning extraction of matrix-matrix multiplies from static analysis of the kernel's code. A comprehensive study of these aspects will be addressed in further work.

5.3. Full-application Study

In this section, we investigate the performance gain for an entire finite element computation developed in Firedrake, a static linear elasticity problem. The source code is available at [Luporini 2014b]. The application simulates ... .
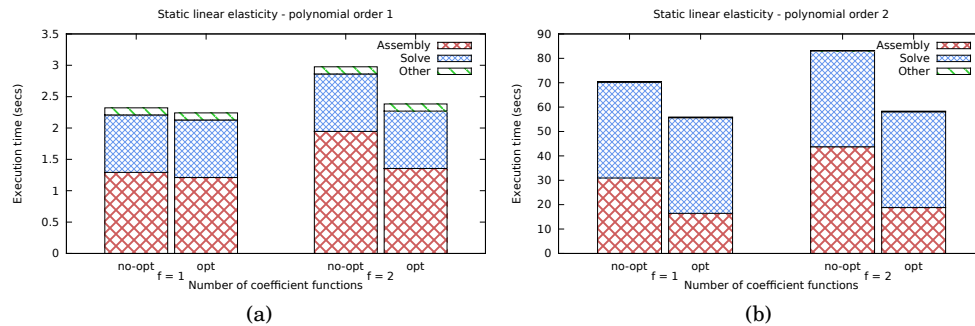
Fig. 10: Performance improvement over non-optimized code for the static linear elasticity equation. The tetrahedral mesh is composed of 196608 elements. Experiments were executed on a single core of a Sandy Bridge architecture.

The execution time of a (non-explicit) finite element method is dominated by two factors: assembly and solve. The evaluation of all local element matrices and vectors, and their insertion, respectively, in a "global" sparse matrix and a global vector, compose the "assembly" phase. The global matrix and vector form a linear system, usually solved by an iterative method; this is the "solve" phase. The percentage of time spent in assembly and solve varies from problem to problem. As reiterated in the available literature, for example in [Olgaard and Wells 2010], the computational cost of local assembly grows with the *complexity* of the partial differential equation (e.g. because of larger loops and more articulated expressions), while the solve time increases with polynomial order and mesh discretization. The complexity of an equation depends on several factors, including the number of derivatives and coefficient functions (i.e. additional known functions that characterize the equation).

We study two versions of the static linear elasticity problem: 1) with one coefficient function, $f = 1$, and 2) with two coefficient functions, $f = 2$. More coefficient functions are also plausible; however, as we will see, the assembly process starts being particularly expensive already with $f = 1$. For each of these two versions, we examine the cases of polynomial order $p = 1$ and $p = 2$. To run our experiments, we use a single core of the Sandy Bridge architecture described in Section 5. The application runs on a tetrahedral mesh composed of 196608 elements.

In Figure 10, we show the execution times for the four test cases, split over two figures (one for each polynomial order), without and with optimizations enabled. A stacked bar captures the time spent in the assembly phase (assembly), in solving the linear system (solve), and in the other various parts of the program (other - for example, setup of the problem and initialization of the coefficient functions). The *non-opt* and *opt* bars correspond, respectively, to the cases in which no optimizations and a combination of optimizations have been applied. The optimizations applied are generalized loop-invariant code motion, alignment and padding, and expression splitting. We recall that the cost of the insertion of the computed local element matrices (and vectors) in the global matrix (vector) is incorporated in assembly.

We first notice that, in the scenario $[f = 1, p = 1]$, the assembly is dominated by matrix insertion: despite the application of several transformations, only a minimal performance gain is achieved. This changes instantly moving to $p = 2$ and $f = 2$. In these scenarios, not only the cost of assembly becomes larger with respect to solve, but also does it make insertion cost negligible. In such cases, the transformations automatically

applied by COFFEE successfully decrease the impact of assembly over solve. Interesting is the fact that generalized loop-invariant code motion was particularly invasive, with 23 temporaries generated and several redundancies discovered (see Section 3.2).

In these experiments, we observe a maximum performance improvement of $1.47\times$ over the non-optimized local assembly code, obtained in the case $[f = 2, p = 2]$. However, we reiterate the fact that full-application speed ups rise proportionally with the amount of time spent in assembly and, therefore, with the complexity of the equation. By increasing polynomial order and number of coefficient functions, or by simply studying a different, more complex equation, it is our experience that performance gains become increasingly more relevant. The choice of studying the static linear elasticity equation was to show that even relatively simple problems can be characterized by a large proportion of execution time spent in assembly.

6. GENERALITY OF THE APPROACH AND APPLICABILITY TO OTHER DOMAINS

We have demonstrated that our optimizations for cross-loop arithmetic intensity are effective in the context of automated code generation for finite element local assembly. In this section, we discuss about the potential for their applicability in other computational domains and, more in general, to what extent a general-purpose compiler could integrate some of them.

We observe that our choice was to develop COFFEE as a separate, self-contained software module, with clear input/output interfaces, rather then incorporating it within PyOP2. This was motivated by two critical aspects.

Separation of concerns. We believe that in domain-specific frameworks there must be a clear, logical separation of roles reflecting the various levels of abstractions, with domain-specialists that can completely abstract from performance optimization. In Firedrake, for instance, COFFEE decouples the mathematical specification of a finite element method, captured by the Unified Form Language and the FEniCS Form Compiler, from code optimization. This is of fundamental importance to maximize productivity by allowing scientists to focus only on their area of expertise. Practically speaking, from the perspective of the domain-specific language and compiler designers, our optimization strategy represents an incentive to produce extremely simple representations of the code (e.g. fully-inlined mathematical expressions in the form of an abstract syntax tree, in the case of Firedrake) so as to make the architecture-aware code optimizer completely responsible for choosing and applying the most suitable set of transformations.

Generalization to other domains. There are neither conceptual nor technical reasons for which our compiler could not be used outside of the Firedrake system. For example, integration with the popular FEniCS framework, the pioneer of automated code generation for finite element local assembly, would be relatively easy to achieve. More challenging is to assess the generality of our optimization strategy; that is, if and how COFFEE and its transformations are transferable to other computational domains, perhaps other DSLs, and to what extent this would be helpful for improving full-application performance. To answer these questions, we first need to go back to the origins of our compiler. The starting point of our work was the mathematical formulation of a local assembly operation, expressible as follows

$$\forall_{i,j} \quad A_{ij}^K = \sum_{q=1}^{n_1} \sum_{k=1}^{n_2} \alpha_{k,q}(a', b', c', ...)\beta_{q,i,j}(a, b, c, d, ...)\gamma_q(w_K, z_K) \tag{2}$$

The expression represents the numerical evaluation of an integral at n_1 points in the mesh element K to compute the local element matrix A. Functions α, β and γ are problem-specific and can be intricately complex, involving for example the evaluation of derivatives. Abstracting from the inherent structure of α, β and γ, a number of aspects can be highlighted

Optimizing mathematical expressions. Expression manipulation at the mathematical layer (e.g. simplification, decomposition into sub-expressions) opens multiple semantically-equivalent code generation opportunities, characterized by different trade-offs in parallelism, redundant computation, and data locality. The basic idea is to exploit properties of arithmetic operators, like associativity and commutativity, to re-schedule the computation suitably for the underlying architecture. Loop-invariant code motion and expression splitting follow this principle, so they can be re-adapted or extended to any domain computationally similar to local assembly, like those involving tensor contractions [Hartono et al. 2009]. We highlight three notable points.

(1) In Equation 2, the summations correspond to reduction loops, whereas loops over indices i and j are fully parallel. Throughout the paper we assumed to have a single thread per kernel, although it is worth noting that for certain architectures (e.g. GPUs) this could be prohibitive due to memory requirements. Intra-kernel parallelization is one possible solution: a domain-specific compiler like COFFEE could map mathematical quantifiers and operators to different parallelization schemes, and transform both the kernel and the function calling it for multi-threaded execution. This approach is fundamental if performance portability needs to be achieved. We believe that analogous considerations apply to different computational domains.

(2) The various sub-expressions in β only depend on (i.e. iterate along) a subset of the enclosing loops. In addition, some of these sub-expressions might reduce to the same values as iterating along certain iteration spaces. This code structure motivated the generalized loop-invariant code motion technique. The intuition is that whenever sub-expressions invariant with respect to different sets of affine loops can be identified, the question of whether, where and how to hoist them, while minimizing redundant computation, arises.

(3) Associative arithmetic operators are the prerequisite for expression splitting. In essence, this transformation concerns resource-aware execution. It is indeed true that, in the context of COFFEE, expression splitting has been successfully applied to improve register pressure; nevertheless, the basic idea is far more general, which is re-scheduling (re-associating) operations to optimize for some generic parameters. It could be used, for example, as a starting point to perform kernel fission; that is, splitting a kernel into multiple parts, each part characterized by less stringent memory requirements (a variant of this idea for non-affine loops in unstructured mesh applications has been adopted in [Bertolli et al. 2013]). In Equation 2, for instance, not only any of the functions α, β and γ could be split (assuming they include associative operators), but also the evaluation of α could be completely extracted and evaluated in a separate kernel: this would avoid allocating space for $[a', b', c', ...]$ in a second kernel computing the rest of the expression. This may be particularly indicated for many-core architectures in which the available per-core memory is much smaller than that in traditional CPUs.

Code generation and applicability of the transformations. All array sizes and loop bounds, like $n1$ and $n2$ in Equation 2, are known at code generation time. This means that "good" code can be generated. For example, loop bounds can be made explicit, arrays can be statically initialized, and pointer aliasing is easily avoidable. Further, all

of these factors contribute to the applicability and the effectiveness of all of our code transformations. For instance, knowing loop bounds allows both generating correct code when applying vector-register tiling (see Section 3.3) and discovering redundant computation opportunities (see Section 3.2). On the other hand, the padding and data alignment transformation could be performed directly at run-time; note that, theoretically, it could also be automated by a general-purpose compiler though profile-guided optimization, provided that some sort of data-flow analysis is performed to ensure that the extra loop iterations over the padded region do not affect the numerical results.

Multi-loop vectorization. Compiler auto-vectorization has become effective for a variety of codes. Nevertheless, multi-loop vectorization, which involves loading and storing data along a subset of the loops characterizing the iteration space (rather than just along the innermost loop), is not supported by available general-purpose and polyhedral compilers to the best of our knowledge. However, the outer-product vectorization technique presented in this paper shows that two-loop vectorization can outperform standard auto-vectorization; more importantly, we expect the performance gain to scale with the number of vectorized loops and the vector length (as proved by the Xeon Phi results). Despite being not straightforward to automate multi-loop vectorization in a general-purpose compiler, especially if stencils are present, we believe that in specific domains this could be more easily achieved. The intuition is to map the memory access pattern on vector registers, and then relying on in-register shuffling to minimize the traffic between memory and processor.

7. RELATED WORK

The finite element method is extensively used to approximate solutions of PDEs. Well-known frameworks and applications include nek5000 [Paul F. Fischer and Kerkemeier 2008], the FEniCS project [Logg et al. 2012], Fluidity [AMCG 2010], and of course Firedrake. Numerical integration is usually employed to implement the local assembly phase. The recent introduction of domain specific languages (DSLs) to decouple the finite element specification from its underlying implementation facilitated, however, the development of novel approaches. Methods based on tensor contraction [Kirby and Logg 2006] and symbolic manipulation [Russell and Kelly 2013] have been implemented. We have designed COFFEE to specifically target numerical integration because it has been demonstrated that it remains the optimal choice for a wide class of problems [Olgaard and Wells 2010].

Optimization of local assembly using numerical integration for CPU platforms has been addressed in FEniCS [Olgaard and Wells 2010]. The comparison between COFFEE and this work is presented in Section 5.2.7. In [Markall et al. 2010], and more recently in [Knepley and Terrel 2013], the problem has been studied for GPU architectures. In [Kruel and Bana 2013], variants of the standard numerical integration algorithm have been specialized and evaluated for the PowerXCell processor, but an exhaustive study from the compiler viewpoint - like ours - is missing, and none of the optimizations presented in Section 3 are mentioned. Among these efforts, to the best of our knowledge, COFFEE is the first work targeting low-level optimizations through a real compiler approach.

Our compiler-based optimization approach is made possible by the top-level DSL, which enables automated code generation. DSLs have been proven successful in auto-generating optimized code for other domains: Spiral [Püschel et al. 2005] for digital signal processing numerical algorithms, [Spampinato and Püschel 2014] for dense linear algebra, or Pochoir [Tang et al. 2011] and SDSL [Henretty et al. 2013] for image processing and finite difference stencils. Similarly, PyOP2 is used by Firedrake

to express iteration over unstructured meshes in scientific codes. COFFEE improves automated code generation in Firedrake.

Many code generators, like those based on the Polyhedral model [Bondhugula et al. 2008] and those driven by domain-knowledge [Stock et al. 2011], make use of cost models. The alternative of using auto-tuning to select the best implementation for a given problem on a certain platform has been adopted by nek5000 [Shin et al. 2010] for small matrix-matrix multiplies, the ATLAS library [Whaley and Dongarra 1998], and FFTW [Frigo et al. 2005] for fast fourier transforms. In both cases, pruning the implementation space is fundamental to mitigate complexity and overhead. Likewise, COFFEE uses a cost model and heuristics (Section 4) to steer the optimization process.

8. CONCLUSIONS

In this paper, we have presented the design, optimizations and systematic performance evaluation of COFFEE, a compiler for finite element local assembly. In this context, to the best of our knowledge, COFFEE is the first compiler capable of introducing low-level optimizations to maximize instruction-level parallelism, register locality and SIMD vectorization. Assembly kernels have particular characteristics. Their iteration space is usually very small, with the size depending on aspects like the degree of accuracy one wants to reach (polynomial order of the method) and the mesh discretization employed. The data space, in terms of number of arrays and scalars required to evaluate the element matrix, grows proportionally with the complexity of the finite element problem. COFFEE has been developed taking into account all of these degrees of freedom, based on the idea that reducing the problem of local assembly optimization to a fixed sequence of transformations is far too superficial if close-to-peak performance needs to be reached. The various optimizations overcome limitations of current vendor and research compilers. The exploitation of domain knowledge allows some of them to be particularly effective, as demonstrated by our experiments on two state-of-the-art Intel platforms. Further work includes a comprehensive study about feasibility and constraints on transforming kernels into a sequence of calls to external linear algebra libraries. COFFEE supports all of the problems expressible in Firedrake, and is already integrated with this framework. The generality and the applicability of the proposed code transformations to other domains has also been discussed.

REFERENCES

M. S. Alnæs, A. Logg, K. B. Ølgaard, M. E. Rognes, and G. N. Wells. 2014. Unified Form Language: A domain-specific language for weak formulations of partial differential equations. *ACM Trans Math Software* 40, 2, Article 9 (2014), 9:1–9:37 pages. DOI:http://dx.doi.org/10.1145/2566630

AMCG. 2010. *Fluidity Manual* (version 4.0-release ed.). Applied Modelling and Computation Group, Department of Earth Science and Engineering, South Kensington Campus, Imperial College London, London, SW7 2AZ, UK. available at http://hdl.handle.net/10044/1/7086.

C. Bertolli, A. Betts, N. Loriant, G.R. Mudalige, D. Radford, D.A. Ham, M.B. Giles, and P.H.J. Kelly. 2013. Compiler Optimizations for Industrial Unstructured Mesh CFD Applications on GPUs. In *Languages and Compilers for Parallel Computing*, Hironori Kasahara and Keiji Kimura (Eds.). Lecture Notes in Computer Science, Vol. 7760. Springer Berlin Heidelberg, 112–126. DOI:http://dx.doi.org/10.1007/978-3-642-37658-0_8

Uday Bondhugula, Albert Hartono, J. Ramanujam, and P. Sadayappan. 2008. A Practical Automatic Polyhedral Parallelizer and Locality Optimizer. In *Proceedings of the 2008 ACM SIGPLAN Conference on Programming Language Design and Implementation (PLDI '08)*. ACM, New York, NY, USA, 101–113. DOI:http://dx.doi.org/10.1145/1375581.1375595

Zachary DeVito, Niels Joubert, Francisco Palacios, Stephen Oakley, Montserrat Medina, Mike Barrientos, Erich Elsen, Frank Ham, Alex Aiken, Karthik Duraisamy, Eric Darve, Juan Alonso, and Pat Hanrahan. 2011. Liszt: A Domain Specific Language for Building Portable Mesh-based PDE Solvers. In *Proceedings of 2011 International Conference for High Performance Computing, Networking, Storage and Analysis (SC '11)*. ACM, New York, NY, USA, Article 9, 12 pages. DOI:http://dx.doi.org/10.1145/2063384.2063396

Firedrake contributors. 2014. The Firedrake Project. http://www.firedrakeproject.org. (2014).

Matteo Frigo, Steven, and G. Johnson. 2005. The design and implementation of FFTW3. In *Proceedings of the IEEE*. 216–231.

Albert Hartono, Qingda Lu, Thomas Henretty, Sriram Krishnamoorthy, Huaijian Zhang, Gerald Baumgartner, David E. Bernholdt, Marcel Nooijen, Russell Pitzer, J. Ramanujam, and P. Sadayappan. 2009. Performance Optimization of Tensor Contraction Expressions for Many-Body Methods in Quantum Chemistry. *The Journal of Physical Chemistry A* 113, 45 (2009), 12715–12723. DOI:http://dx.doi.org/10.1021/jp9051215 PMID: 19888780.

Tom Henretty, Richard Veras, Franz Franchetti, Louis-Noël Pouchet, J. Ramanujam, and P. Sadayappan. 2013. A Stencil Compiler for Short-vector SIMD Architectures. In *Proceedings of the 27th International ACM Conference on International Conference on Supercomputing (ICS '13)*. ACM, New York, NY, USA, 13–24. DOI:http://dx.doi.org/10.1145/2464996.2467268

Intel Corporation. 2012. *Intel architecture code analyzer (IACA)*. [Online]. Available: http://software.intel.com/en-us/articles/intel-architecture-code-analyzer/.

Robert C. Kirby, Matthew Knepley, Anders Logg, and L. Ridgway Scott. 2005. Optimizing the Evaluation of Finite Element Matrices. *SIAM J. Sci. Comput.* 27, 3 (Oct. 2005), 741–758. DOI:http://dx.doi.org/10.1137/040607824

Robert C. Kirby and Anders Logg. 2006. A Compiler for Variational Forms. *ACM Trans. Math. Softw.* 32, 3 (Sept. 2006), 417–444. DOI:http://dx.doi.org/10.1145/1163641.1163644

Matthew G. Knepley and Andy R. Terrel. 2013. Finite Element Integration on GPUs. *ACM Trans. Math. Softw.* 39, 2, Article 10 (Feb. 2013), 13 pages. DOI:http://dx.doi.org/10.1145/2427023.2427027

Filip Kruel and Krzysztof Bana. 2013. Vectorized OpenCL Implementation of Numerical Integration for Higher Order Finite Elements. *Comput. Math. Appl.* 66, 10 (Dec. 2013), 2030–2044. DOI:http://dx.doi.org/10.1016/j.camwa.2013.08.026

Anders Logg, Kent-Andre Mardal, Garth N. Wells, and others. 2012. *Automated Solution of Differential Equations by the Finite Element Method*. Springer. DOI:http://dx.doi.org/10.1007/978-3-642-23099-8

Fabio Luporini. 2014a. Helmholtz, Advection-Diffusion, and Burgers UFL code. https://github.com/firedrakeproject/firedrake/tree/pyop2-ir-perf-eval/tests/perf-eval. (2014).

Fabio Luporini. 2014b. Static linear elasticity code. https://github.com/firedrakeproject/firedrake-bench/tree/experiments/elasticity. (2014).

Graham R. Markall, David A. Ham, and Paul H.J. Kelly. 2010. Towards generating optimised finite element solvers for {GPUs} from high-level specifications. *Procedia Computer Science* 1, 1 (2010), 1815 – 1823. DOI:http://dx.doi.org/10.1016/j.procs.2010.04.203 {ICCS} 2010.

G. R. Markall, F. Rathgeber, L. Mitchell, N. Loriant, C. Bertolli, D. A. Ham, and P. H. J. Kelly. 2013. Performance portable finite element assembly using PyOP2 and FEniCS. In *Proceedings of the International Supercomputing Conference (ISC) '13 (Lecture Notes in Computer Science)*, Vol. 7905. In press.

Kristian B. Olgaard and Garth N. Wells. 2010. Optimizations for quadrature representations of finite element tensors through automated code generation. *ACM Trans. Math. Softw.* 37, 1, Article 8 (Jan. 2010), 23 pages. DOI:http://dx.doi.org/10.1145/1644001.1644009

James W. Lottes Paul F. Fischer and Stefan G. Kerkemeier. 2008. nek5000 Web page. (2008). http://nek5000.mcs.anl.gov.

Markus Püschel, José M. F. Moura, Jeremy Johnson, David Padua, Manuela Veloso, Bryan Singer, Jianxin Xiong, Franz Franchetti, Aca Gacic, Yevgen Voronenko, Kang Chen, Robert W. Johnson, and Nicholas Rizzolo. 2005. SPIRAL: Code Generation for DSP Transforms. *Proceedings of the IEEE, special issue on "Program Generation, Optimization, and Adaptation"* 93, 2 (2005), 232– 275.

Florian Rathgeber, Graham R. Markall, Lawrence Mitchell, Nicolas Loriant, David A. Ham, Carlo Bertolli, and Paul H.J. Kelly. 2012. PyOP2: A High-Level Framework for Performance-Portable Simulations on Unstructured Meshes. In *High Performance Computing, Networking, Storage and Analysis (SCC), 2012 SC Companion:*. 1116–1123. DOI:http://dx.doi.org/10.1109/SC.Companion.2012.134

I. Z. Reguly, E. László, G. R. Mudalige, and M. B. Giles. 2007. Vectorizing Unstructured Mesh Computations for Many-core Architectures. In *Proceedings of Programming Models and Applications on Multicores and Manycores (PMAM'14)*. ACM, New York, NY, USA, Article 39, 12 pages. DOI:http://dx.doi.org/10.1145/2560683.2560686

Diego Rossinelli, Babak Hejazialhosseini, Panagiotis Hadjidoukas, Costas Bekas, Alessandro Curioni, Adam Bertsch, Scott Futral, Steffen J. Schmidt, Nikolaus A. Adams, and Petros Koumoutsakos. 2013. 11 PFLOP/s Simulations of Cloud Cavitation Collapse. In *Proceedings of the International Conference on High Performance Computing, Networking, Storage and Analysis (SC '13)*. ACM, New York, NY, USA, Article 3, 13 pages. DOI:http://dx.doi.org/10.1145/2503210.2504565

Francis P. Russell and Paul H. J. Kelly. 2013. Optimized Code Generation for Finite Element Local Assembly Using Symbolic Manipulation. *ACM Trans. Math. Software* 39, 4 (2013).

Jaewook Shin, Mary W. Hall, Jacqueline Chame, Chun Chen, Paul F. Fischer, and Paul D. Hovland. 2010. Speeding Up Nek5000 with Autotuning and Specialization. In *Proceedings of the 24th ACM International Conference on Supercomputing (ICS '10)*. ACM, New York, NY, USA, 253–262. DOI:http://dx.doi.org/10.1145/1810085.1810120

Daniele G. Spampinato and Markus Püschel. 2014. A Basic Linear Algebra Compiler. In *International Symposium on Code Generation and Optimization (CGO)*.

Kevin Stock, Tom Henretty, Iyyappa Murugandi, P. Sadayappan, and Robert Harrison. 2011. Model-Driven SIMD Code Generation for a Multi-resolution Tensor Kernel. In *Proceedings of the 2011 IEEE International Parallel & Distributed Processing Symposium (IPDPS '11)*. IEEE Computer Society, Washington, DC, USA, 1058–1067. DOI:http://dx.doi.org/10.1109/IPDPS.2011.101

Yuan Tang, Rezaul Alam Chowdhury, Bradley C. Kuszmaul, Chi-Keung Luk, and Charles E. Leiserson. 2011. The Pochoir Stencil Compiler. In *Proceedings of the Twenty-third Annual ACM Symposium on Parallelism in Algorithms and Architectures (SPAA '11)*. ACM, New York, NY, USA, 117–128. DOI:http://dx.doi.org/10.1145/1989493.1989508

Peter E. J. Vos, Spencer J. Sherwin, and Robert M. Kirby. 2010. From H to P Efficiently: Implementing Finite and Spectral/Hp Element Methods to Achieve Optimal Performance for Low- and High-order Discretisations. *J. Comput. Phys.* 229, 13 (July 2010), 5161–5181. DOI:http://dx.doi.org/10.1016/j.jcp.2010.03.031

R. Clint Whaley and Jack J. Dongarra. 1998. Automatically Tuned Linear Algebra Software. In *Proceedings of the 1998 ACM/IEEE Conference on Supercomputing (Supercomputing '98)*. IEEE Computer Society, Washington, DC, USA, 1–27. http://dl.acm.org/citation.cfm?id=509058.509096